

Physica Scripta

An International Journal for Experimental and Theoretical Physics

Dear

Please find attached a PDF of your article that has appeared in issue _____ of Physica Scripta. This file has been optimised for viewing on screen, but can be printed off. If you would like a version of this file, optimised for printing, or would like to purchase a number of printed copies of your paper, please contact me.

Best Wishes,

Audrey Samuels

Journal Controller

Marston Digital

Omega Park

Collet

Didcot

OX11 7AW

email: samuelsa@lrl.com

voice: +44 1235 518700

fax: +44 1235 515777

web: <http://www.physica.org>

Editorial office

Physica Scripta
The Royal Swedish Academy of Sciences
Box 50005
S-104 05 Stockholm, Sweden

Telephone

+46-(0)8-673 95 00

Telefax

+46-(0)8-673 95 90

Electronic Mail

physica@kva.se

Home Page

<http://www.physica.org>

Site-Specific Neutralization of Slow Multicharged Ions Incident on Solid Surfaces

F. W. Meyer*, H. F. Krause, V. A. Morozov**, C. R. Vane and L. I. Vergara

¹Physics Division, Oak Ridge National Laboratory, Oak Ridge, Tennessee 37831-6372 USA

Received September 11, 2003; accepted November 8, 2003

PACS Ref: 79.20.Rf, 79.20.Ap, 34.50.Dy, 61.18.Bn

Abstract

Recent measurements of projectile neutralization during 120° binary collision backscattering from Au(110) and RbI(100), performed at the ORNL Multicharged Ion Research Facility, are described. A common feature of the Au(110) and RbI(100) results is that the observed scattered charge state distributions show significant dependences on the target azimuthal orientation, even for normal or close to normal incidence conditions. The observed target azimuth dependences originate in part from the fact that for the 120° backscattering geometry, quasi-binary double collisions make significant contributions to the total binary scattering collision flux. For the Au(110) target, the types of possible quasi-binary collisions vary with target azimuth because of the corrugation of the reconstructed surface and the number of layers of atoms exposed in a (110) fcc lattice. For the RbI(100) surface, quasi-binary collisions vary with azimuth because of the ordered, two-component nature of the surface even when scattering from deeper layers is blocked. Sample data for few-keV incident F, Ne, and Ar multicharged incident projectiles are presented to illustrate the underlying concepts.

1. Introduction

In this article a brief overview is given of recent studies of projectile neutralization during large-angle backscattering interactions with metal and insulator surfaces carried out at the ORNL Multicharged Ion Research Facility. In contrast to measurements of projectile neutralization during grazing surface interactions [1] which involve a large number of lattice sites, our backscattering studies have as one of their goals improved understanding of projectile neutralization in the limit of one or two surface-atom collisions. As shown in published results [2,3] for Au(110), such collisions can be identified by energy loss analysis of the scattered projectiles to select binary and quasi-binary collisions. It was further shown that information about projectile neutralization at several different distinguishable surface lattice sites could be obtained from analysis of the target azimuth dependences observed for the various scattered charge states. Due to the surface corrugation of the reconstructed Au(110) surface, scattering from surface atoms on the corrugation ridges, sidewalls, and valleys each resulted in unique characteristic azimuth variations which could be deconvoluted using classical trajectory Monte Carlo simulations. In this manner, projectile neutralization during true binary and quasi-binary double collisions with three different surface lattice sites could be determined [2].

More recently, our projectile neutralization measurements were extended to alkali halide targets, to determine the effect of the significantly reduced electron density

characterizing such targets, and to assess the possibility of resolving the individual target constituents by energy loss analysis. Initial measurements [4] with CsI(100) could not resolve energy losses associated with scattering from the halogen and alkali sites due to the small mass difference of the target atoms. However, subsequent measurements [5] with a RbI(100) target showed clear resolution of halogen and alkali site scattering. This finding opened the door to a site-specific study of neutralization in quasi-binary double collisions, where the identity of the “hard” collision scattering site is determined by energy loss analysis, and the identity of the “soft” collision partner is selected by suitable azimuth orientation of the target relative to the projectile scattering plane. The (100) direction selects an alkali–halogen or halogen–alkali collision sequence, and the $\langle 110 \rangle$ direction a halogen–halogen or alkali–alkali sequence.

In what follows below, both kinds of site-specific projectile neutralization are briefly discussed and illustrated.

2. Experiment

The measurements were performed at the ORNL Multicharged Ion Research Facility (MIRF) [6] using an ultra high vacuum (10^{-10} mbar) apparatus previously described [7]. A chopped primary ion beam is decelerated from $(10 \times q)$ keV to final energies in the range 4–5 keV before impinging on a single crystal Au(110) or RbI(100) surface. The salient features of the two crystal structures and the scattering geometries are indicated schematically in Figs. 1 and 2. The crystal is attached to a goniometer that has two rotational degrees of freedom. A TOF analyzer, located 120° from the incident beam direction, registers projectiles scattered from the crystal surface using a multichannel plate (MCP) detector. The TOF analyzer, which has a floatable drift tube, allows simultaneous measurement of energy distributions and charge fractions for the scattered projectiles [7]. An important feature of this approach is the ability to analyze all scattered charge states, including neutrals, essential for complete determination of scattered charge fractions. Time zero calibration was obtained from the soft X-ray peak registered on the TOF detector resulting from projectile impact on the surface in the case of highly charged ions, or from the secondary electron peak observed when the flight tube and MCP detector were biased a few hundred volts positive. The target surfaces were prepared by cycles of sputter cleaning under grazing incidence conditions using 2 keV Ar^+ ions and successive annealing

*e-mail: meyerfw@ornl.gov

**Now at Infinion Technologies Richmond, Stanton, VA 23150 USA

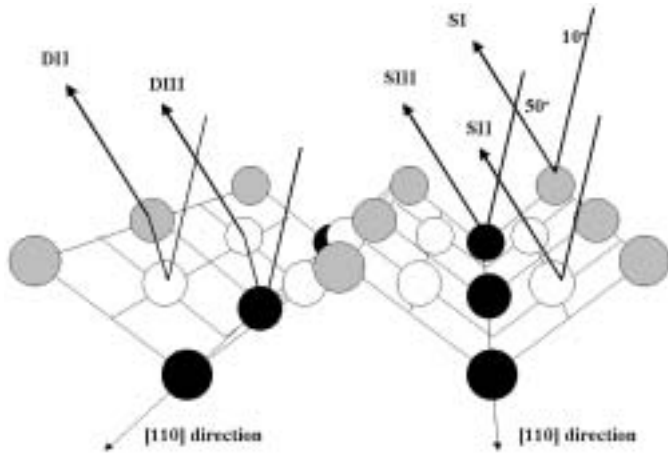


Fig. 1. Schematic diagram of the Au(110) surface, showing the “missing row” reconstruction and the different possible single and quasi-binary backscattering collisions at the surface.

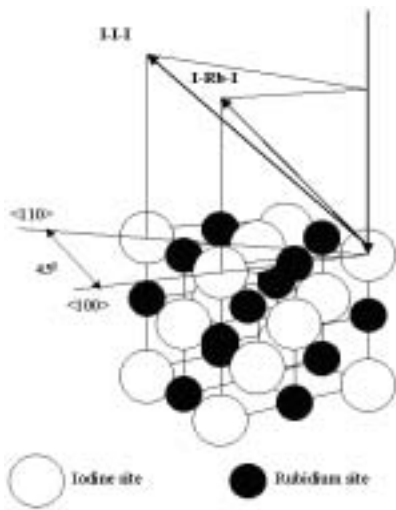


Fig. 2. Schematic diagram of the RbI(100) target, showing the different atomic strings along a $\langle 100 \rangle$ and $\langle 110 \rangle$ direction.

at about 450°C. To prevent macroscopic charging, the RbI target was maintained at a temperature of 250°C during the measurements. The Au(110) measurements were carried out with the sample at room temperature.

The energy-loss technique enables identification of the binary collision partner causing the large-angle backscattering at the surface. When a projectile of energy E_0 with mass m_p elastically scatters from a target atom at rest with mass m_t , the projectile recoil energy E_r depends on the scattering angle θ as [5]

$$E_r = E_0 \left[\frac{\mu \cos \theta + (1 - \mu^2 \sin^2 \theta)^{1/2}}{(1 + \mu)^2} \right], \quad (1)$$

where $\mu = m_p/m_t < 1$. A 120° scattering event (“hard” collision) is associated with a small impact parameter collision (e.g., $b_h \sim 0.133 \text{ \AA}$ for 5 keV Ar projectile incident on Au [3]), and results in a substantial energy loss. Figure 3 shows typical TOF spectra for 4.5 keV Ar¹¹⁺ projectiles 120° backscattered from Au(110) for a range of target azimuth orientations. When the surface has two constituents of significantly different masses (e.g., Rb and I), a hard collision at either site gives rise to different recoil energies that can be resolved experimentally in our TOF apparatus (site-specificity for each final charge state). This is

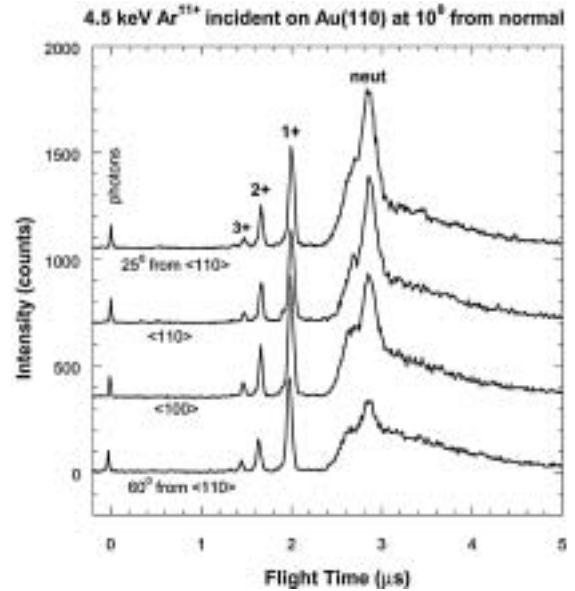


Fig. 3. Measured TOF spectra for 120° backscattered projectiles for 4.5 keV Ar¹¹⁺ projectiles incident on Au(110) at 10° from normal, for four different target azimuth orientations. Note the different binary collision peak areas, particularly for the scattered neutrals at the different azimuths.

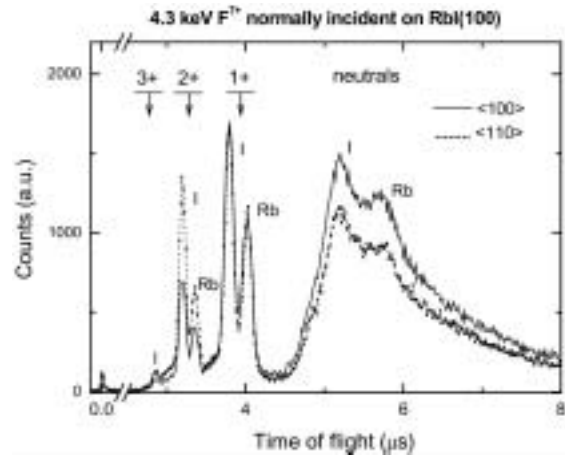


Fig. 4. Measured TOF spectra for 120° backscattered projectiles for 4.3 keV F⁷⁺ projectiles normally incident on RbI(100), for two different azimuths. Note the decreased neutralization evident along a $\langle 110 \rangle$ direction (see text).

illustrated in Fig. 4 for 4.3 keV F⁷⁺ projectiles 120° backscattered from RbI(100) for two different target azimuths.

For a possible subsequent small-angle scattering event (i.e., “soft” collision, $b_s \gg b_h$) on the receding or approach trajectory, very little energy is lost. Therefore, a “quasi-binary” double-scattering event (“hard-soft” or “soft-hard” collision sequence) has an energy loss very close to, and experimentally unresolvable from, that of a single “hard” collision. As a result, the classification and identification of such quasi-binary double collisions is made possible only by analysis of classical trajectory simulations, as described in the following section.

3. Trajectory simulations

To understand the various target orientation dependences of the scattered fluxes, and the types of collisions comprising them, projectile trajectory simulations using

the MARLOWE (versions 14c and 15b) code [8] were carried out. MARLOWE treats the interaction between the projectile and the surface in an elastic binary collision approximation (BCA). An exponential-sum screened Coulomb interaction potential was chosen, and a (2×1) reconstruction of the Au(110) surface was assumed [9]. The primary beam energy distribution was simulated in a series of MARLOWE tasks with different initial particle kinetic energies. Due to computing time constraints the angular acceptance was increased by a factor of 4 over the experimental acceptance angle of 2° . Of the up to 10^8 trajectories generated for each target orientation investigated, about $(0.03\text{--}0.08)\%$ were scattered into the detector acceptance cone. For all interactions resulting in backscattering from the surface, the number of collisions, scattering angles, etc. were saved, permitting their subsequent reconstruction.

The simulations were used as the basis for analyzing the collision events contributing to the “binary collision” (BC) peak seen experimentally. They reveal that the BC peak is in fact built up from two kinds of events—pure single SC and “quasi-binary” double DC collisions. In the case of the Au(110) surface, the quasi-binary DC events are particularly prominent for scattering along the [100] target azimuth direction, i.e. *across* the missing rows of the reconstructed Au(110) surface, as is illustrated in Fig. 5. Higher multiplicity events (i.e. number of collisions > 2) do not contribute to the BC peak, and form instead the pedestal upon which the peak sits. This multiple collision background has a somewhat different shape in the case of the RbI(100) target, as illustrated in Fig. 6. The more prominent difference between the two simulated spectra is the presence of two peaks for the RbI(100) target, at the expected energy for binary collisions with the Rb and I constituent atoms of the alkali halide crystal. The ratio of the Rb and I collision peak areas corresponds closely to the calculated ratio of the relevant differential scattering cross sections for these two atomic species at 120° , i.e. about 70%. For both targets, the relative contributions of true binary and quasi-binary double (and at higher energy, triple) collisions to the BC peak vary strongly with target azimuth, and underlie the measured azimuth variations of scattered charge fractions that will be shown in a later section. It is important to note that for both targets, for

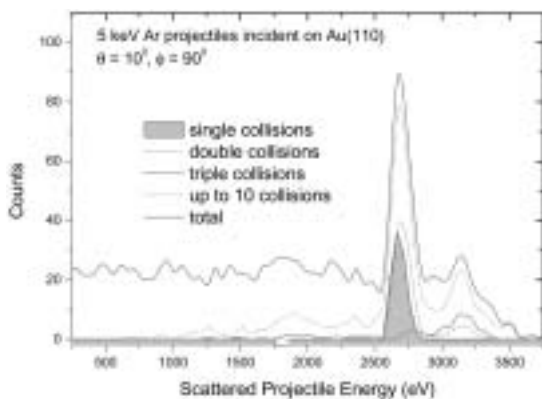


Fig. 5. MARLOWE simulation results for 5 keV Ar projectiles incident on Au(110) along a (100) direction. Note that elastic scattering peak is built up only of single and quasi-binary double collisions.

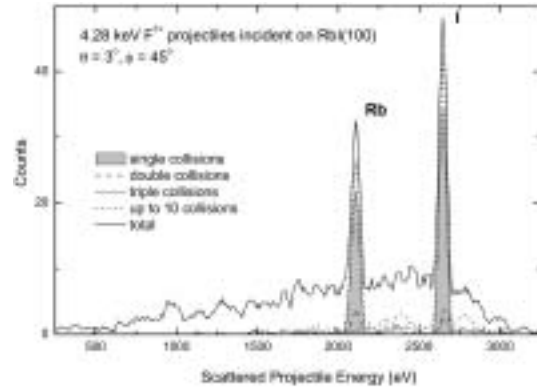


Fig. 6. MARLOWE simulation results for 4.28 keV F projectiles incident on RbI(100) along a (110) direction, showing the dominance of single collisions in the elastic scattering peak for the indicated scattering geometry. Note the resolved elastic scattering peaks for Rb and I lattice sites.

incidence angles close to normal, the simulations indicate that the binary and quasi-binary collisions contributing to the observed backscattering peaks occur almost exclusively at the surface-vacuum interface. In the case of the RbI(100) target this means that only the topmost target layer participates, while in the case of the Au(110) target, the first three layers are involved. The latter arises due to the “missing row” surface reconstruction of the (110) surface, as has been already illustrated in Fig. 1.

4. Results and discussion

4.1. Au(100) target

As can be seen in Fig. 3, for the Au(110) target there are significant variations with target azimuth of the scattered binary collision fluxes, particularly in the case of the neutral yields. The azimuthal variations of the individual scattered charge fractions are shown in greater detail for 5 keV incident Ar^{2+} and Ar^{11+} projectiles in Fig. 7(a). Interestingly, the observed azimuth dependences are different for each scattered charge state, strongly suggesting that the different scattered charge-state fluxes evolved from different ensembles of trajectories. When the scattered binary collision flux is summed over all final charge states, two interesting features are noted, both of which are indicated in Fig. 7(b). First, the two different incident charge states have identical azimuth variations in the total binary collision fluxes. Second, these total binary collision fluxes show excellent agreement with the MARLOWE trajectory simulations discussed above. Also indicated in Fig. 7(b) are the true single collision (SC) and the quasi-binary double collision (DC) contributions making up the total scattered flux. The SC component in turn consists of contributions from only the three exposed layers, **SI**, **SII**, and **SIII**, while the DC component consists of contributions from only the second and third exposed layers, i.e. **DII** and **DIII** as illustrated in Fig. 1. Importantly, each of these 5 collision types has its own characteristic azimuth variation. As shown in Ref. [3] these unique azimuth variations could be used as fitting functions to determine the contribution of each collision type to the different scattered charge state fluxes. The result could then be inverted to obtain neutralization efficiencies for each of the

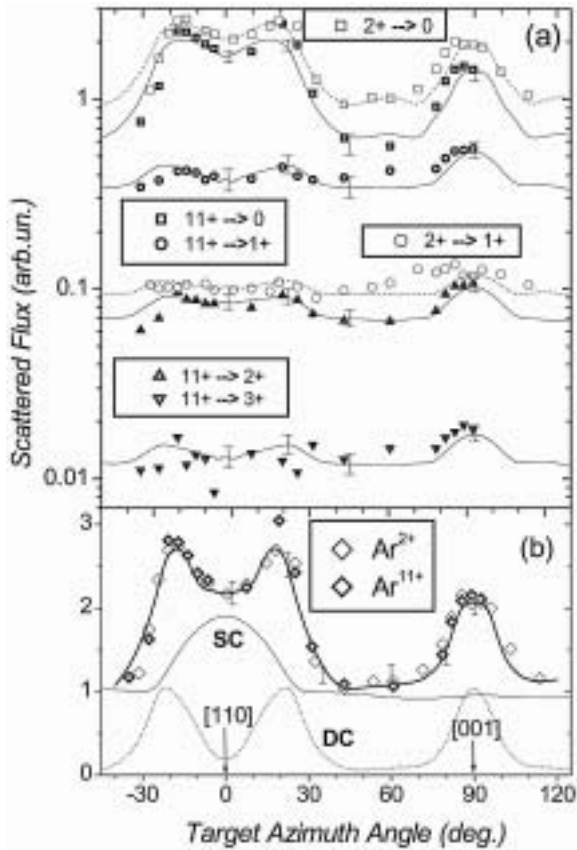


Fig. 7. (a) Azimuth dependences of scattered neutral and charged binary collision fluxes for Ar^{2+} (open symbols) and Ar^{11+} (solid symbols) incident on $\text{Au}(110)$ at 10° ; lines are fits to the data using the MARLOWE simulations (see Ref. 3). (b) Azimuth dependences of the total binary collision fluxes for both incident ions. Also shown are simulation results for single, SC, and quasi-binary double, DC, collisions. Their sum is shown as the thick line.

5 distinct collision types. The neutralization efficiencies for the three true single collision types are summarized in Table I.

4.2. $\text{RbI}(100)$ target

In contrast to the $\text{Au}(110)$ target, where three target layers are active in the binary collision backscattering of the incident projectile, our trajectory simulations show that binary collision backscattering from $\text{RbI}(100)$ occurs predominantly from the topmost layer. Blocking and shadowing effects on the receding trajectory after hard collisions in deeper layers thus do not play a role in determining possible azimuthal variations of the projectile binary collision backscattered flux. As a result, both the simulations and measured spectra show more subtle variations with target azimuth. For normal incidence

Table I. Scattered charge fractions and mean charge for **SI**, **SII**, and **SIII** collisions for 5 keV Ar^{11+} collisions incident on $\text{Au}(110)$ at 10° from normal (see Fig. 1).

Outgoing charge state	SI	SII	SIII
0	0.1	1.0	1.0
1 +	0.75	0.0	0.0
2 +	0.125	0.0	0.0
3 +	0.025	0.0	0.0
Mean scattered charge state	1.01	0.0	0.0

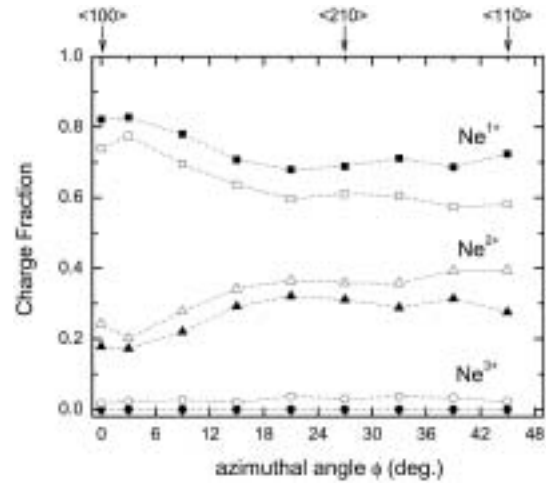


Fig. 8. Azimuth dependence of binary collision scattered charge state fluxes for 5.6 keV Ne^{8+} normally incident on $\text{RbI}(100)$. Note the increased neutralization along the $\langle 100 \rangle$ direction.

projectiles, the observed variation is mainly due to differences in passing distance to the nearest neighbor as the azimuth is varied. Specifically, when changing from the $\langle 100 \rangle$ to the $\langle 110 \rangle$ direction, the nearest neighbor distance changes from 3.66 to 5.17 Å, with a correspondingly greater passing distance to the nearest neighbor on the receding trajectory which leaves the surface at 30° . Figure 8 shows the azimuthal variations of the scattered charge fractions for 5.6 keV normally incident Ne^{8+} projectiles resulting from quasi-binary collision backscattering from Rb and I lattice sites. As the figure suggests, in contrast to the F projectile spectra shown in Fig. 4, the Ne spectra show no discernible binary-collision neutral formation for these conditions. Interestingly, both Rb- and I- backscattered projectile charge states show the same trend with azimuth orientation, i.e., smoothly decreasing degrees of neutralization in going from the $\langle 100 \rangle$ to the $\langle 110 \rangle$ azimuthal direction. The fact that, in changing from the $\langle 100 \rangle$ to the $\langle 110 \rangle$ azimuth, not only the nearest neighbor passing distance changes, but also its identity, thus does not appear to matter in the observed azimuth variation. The fact that there is also a transition from I-Rb, or Rb-I quasi-binary scattering to I-I or Rb-Rb scattering would, in general, be expected to result in different neutralization efficiencies for the Rb and I backscattered projectiles. It is surprising that such differences are not evident in the measured spectra, because the two target species exist in the lattice as I^- and Rb^+ (i.e. since the most loosely bound valence electrons are localized at the I sites), and significant differences are observed between the scattered neutral fractions resulting from highly-charged normally incident Ne and F projectile backscattering.

5. Summary

The origin of the sizable variations in the total scattered binary collision flux and that of the individual scattered charge states in the case of Au target (even in the case of the close to normal incidence conditions discussed here) lies in a rather fortuitous combination of the face-centered-

cubic structure of the target, the (110) surface cut, and the close proximity in values of the 110° opening angle of the surface corrugations and the 120° scattering geometry employed. For backscattered projectiles incident 10° away from normal and backscattered at this angle, quasi-binary scattering from the second and third layers is blocked on the receding trajectory for certain azimuth orientations by lattice sites in the shallower layers. In the vicinity of these shadowing or blocking directions, the receding projectile has higher likelihoods of soft encounters with additional lattice sites which can lead to further neutralization, but, under certain conditions, also to re-ionization, as has already been noted elsewhere [10].

In the case of the RbI(100) surface, the total azimuthal flux variation is much more subtle, since for close to normal incidence, binary collisions with all layers deeper than the surface layer are blocked. Nevertheless, significant azimuth variations in the scattered charge states have been observed. Much more dramatic variations have been observed by changing the incidence angle [11]; these variations are attributed not only to the presence or absence of encounters with nearest neighbors, but also more distant atoms lying along particular directional strings. Importantly, even away from normal incidence, the MARLOWE simulations suggest that subsurface layer contributions to the binary collision flux are not significant. It thus appears that these proximity effects can be studied without the added complexity of competing or distorting effects for deeper layer contributions. In addition, significant variations in scattered neutral fluxes are observed for different incident projectiles, suggesting the importance of level matching effects even for the complex multi-electron transfer processes involved in the large-angle backscattering binary collisions studied here.

So far, observation of dramatic differences between I-Rb, Rb-I, I-I and Rb-Rb quasi-binary scattering have remained elusive. It remains to be determined whether this is due to a mismatch between the relevant capture distances

and the atomic separations in the RbI lattice, injudicious choice of scattering projectiles, energies, scattering geometry, or a combination thereof. Work will continue in this fruitful research area with the hope of elucidating some of these outstanding questions.

Acknowledgements

This research was sponsored in part by the Office of Fusion Energy Sciences and by the Office of Basic Energy Sciences of the U. S. Department of Energy under contract No. DE-AC05-00OR22725 with UT-Battelle, LLC. VAM and LIV were appointed through the ORNL Postdoctoral Research Associates Program administered jointly by Oak Ridge Associated Universities and ORNL.

References

1. Folkerts, L., Schippers, S., Zehner, D. M. and Meyer, F. W., Phys. Rev. Lett. **74**, 2204 (1995); Phys. Rev. Lett. **75**, 983 (1995).
2. Meyer, F. W. and Morozov, V. A., Nucl. Instr. Meth. **B 157**, 297 (1999).
3. Morozov, V. A. and Meyer, F. W., Phys. Rev. Lett. **86**, 736 (2001); Meyer, F. W. and Morozov, V. A., Nucl. Instr. Meth. **B 193**, 530 (2002).
4. Meyer, F. W., Morozov, V. A., Mroghenda, J. and Vane, C. R., Datz, S., Nucl. Instr. Meth. **B 193**, 508 (2002).
5. Meyer, F. W., Krause, H. F. and Vane, C. R., Nucl. Instr. Meth. **B 203**, 231 (2003); Nucl. Instr. Meth. **B 205**, 700 (2003).
6. Meyer, F. W., "ECR-based atomic collision physics research at ORNL MIRROR in: Trapping of Highly Charged Ions: Fundamentals and Applications". (Edited by J. Gillaspay) (Nova Science Pub., New York 2000), p. 117.
7. Morozov, V. A. and Meyer, F. W., Rev. Sci. Instrum. **70**, 4515 (1999).
8. Robinson, M. T., Radiat. Eff. Defect Solid **130**, 3 (1994); Phys. Rev. **B40**, 10717 (1989).
9. Moritz, W. and Wolf, D., Surf. Sci. **88**, L29 (1979); Koch, R. *et al.*, Appl. Phys. **A 55**, 417 (1992).
10. Morozov, V. A. and Meyer, F. W., Physica Scripta **T92**, 31 (2001).
11. Vergara, L. I., Krause, H. F. and Meyer, F. W., to be published in Surf. Coat. Techn. (2004).